

Connectome harmonics track EEG network dynamics on a subsecond time scale

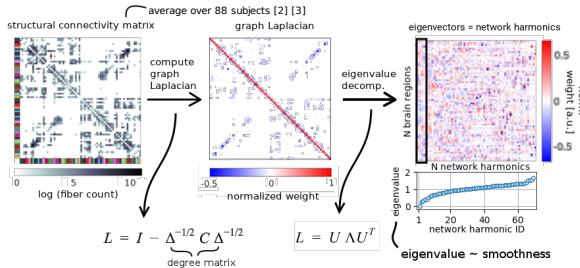
Similar to LSD Harmonic research (look Oral Awareness Consciousness Harmonic notes)

Katharina Glomb (1), Joan Rue Queralt (1,2), David Pascucci (2), Michaël Defferrard (3), Sébastien Tourbier (1), Margherita Carboni (4,5), Maria Rubega (6), Serge Vulliemoz (4), Gijs Plomp (2), Patric Hagmann (1)

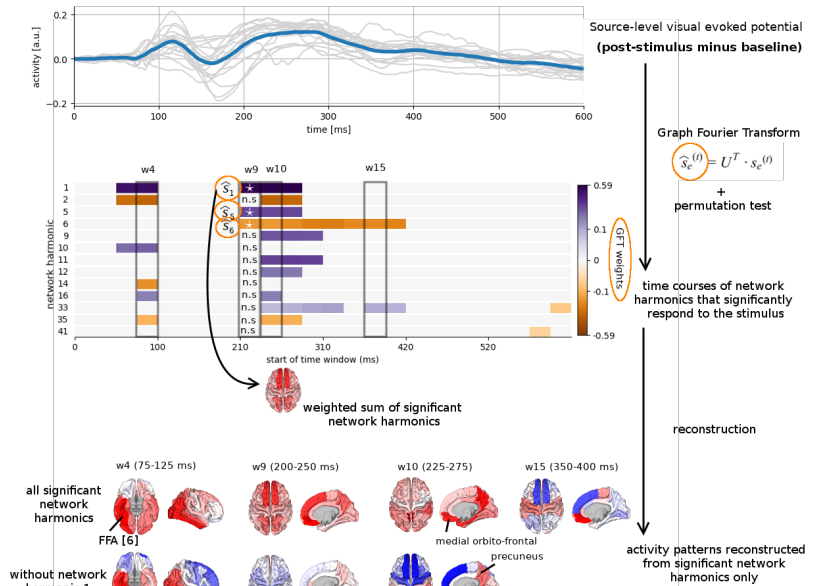
1 Connectomics Lab, Dept. of Radiology, University Hospital of Lausanne and University of Lausanne (CHUV-UNIL), Lausanne, Switzerland; 2 Perceptual Networks Group, Dept. of Psychology, University of Fribourg, Fribourg, Switzerland; 3 Signal Processing Lab 2, EPFL, Lausanne, Switzerland; 4 EEG and Epilepsy, Neurology, University Hospitals of Geneva and University of Geneva, Geneva, Switzerland; 5 Functional Brain Mapping Lab, Department of Fundamental Neuroscience, University of Geneva, Geneva, Switzerland; 6 Neuromove-Rehab Lab, University of Padova, Padova, Italy

video: <https://tinyurl.com/y72o7rsy>

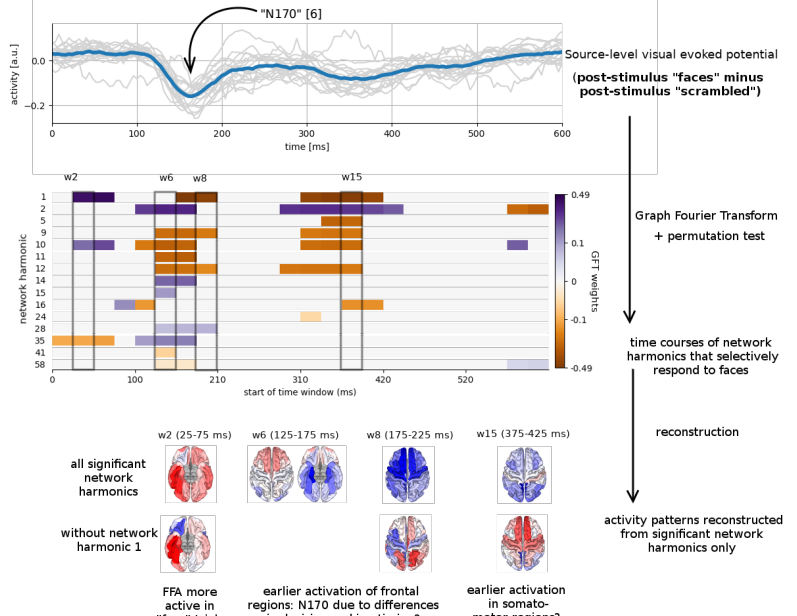
1 Obtaining network harmonics [1]



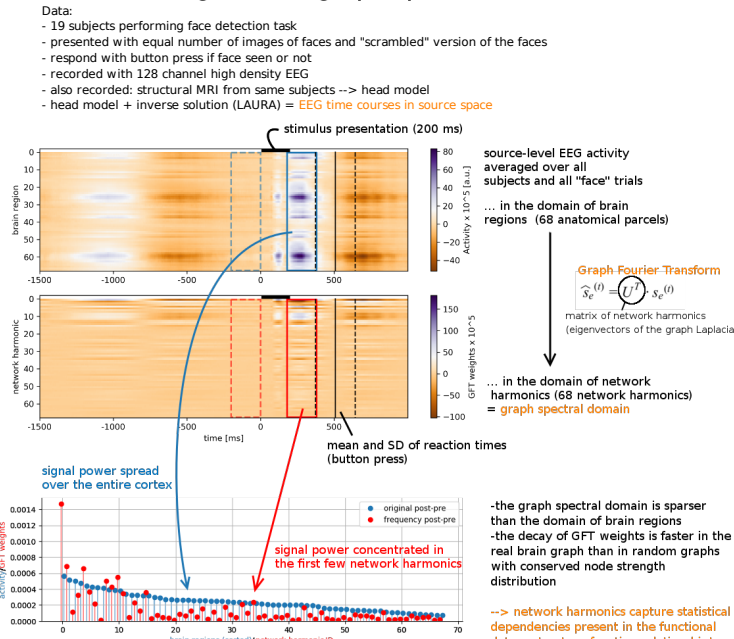
3 Tracking of fast network dynamics



4 Capturing the difference between conditions



3 Transforming into the graph spectral domain



Take home messages

We show a fast, simple, multimodal approach to tracking large-scale dynamics in the brain on a subsecond time scale.

Network harmonics provide a sparse basis in which to represent the EEG signal. This means that the way in which they capture the SC structure is meaningful for functional data:

integration and segregation on multiple scales
ordering by smoothness
modular structure is not fixed

Our method is statistically powerful and can potentially be applied to any task without prior knowledge of where effects should be expected

References

- [1] Hagmann et al., 2013, IEEE signal processing magazine
- [2] Griffa et al., 2019, Zenodo (dataset)
- [3] Hagmann et al., 2008, PLoS biology
- [4] Alayrac et al., 2016, Nature Communications
- [5] Defferrard et al., 2017, <https://github.com/epfl-lts/pygsp> (2017)
- [6] Eimer, 2000, NeuroReport



Extracting Beat Information in Sleeping Brain

Yan Wang^{2,3†}, Yuanye Wang^{1†}, Qihong Zou², Jia-Hong Gao^{2*}, Huan Luo^{1*}



¹ School of Psychological and Cognitive Sciences, Peking University, Beijing 100871, China

² Center for MRI Research, Academy for Advanced Interdisciplinary Studies, Peking University, Beijing 100871, China

³ Chinese Institute for Brain Research, Beijing 102206, China

Contact me:
yanw@pku.edu.cn

INTRODUCTION

- Beat has been revealed to involve dynamic communication between auditory cortex and brain regions for motor planning (Morillon, B et al., 2014).
- Beat perception has been suggested to occur in a relatively automatic manner, it remains unknown whether and how the brain extracts rhythmic auditory information during non-rapid eye movement (NREM) sleep.
- In the present study, we employed an auditory sequence paradigm in combination with a time-resolved general linear modelling (GLM) analysis and EEG recordings to investigate beat processing during awake and sleep states.

METHODS

- **Paradigm.** Here we used an adapted experiment paradigm (Benjamin Morillon and Sylvain Baillet, 2017) to investigate how the beat information modulates and shapes the neuronal activities over time.
- **Participants:** 21 healthy university students.
- **Data Analysis.** To dissociate the modulation by rhythm, frequency and loudness, we used a time-resolved GLM analysis on the EEG response for each tone stimuli during sleep and wakefulness, respectively.

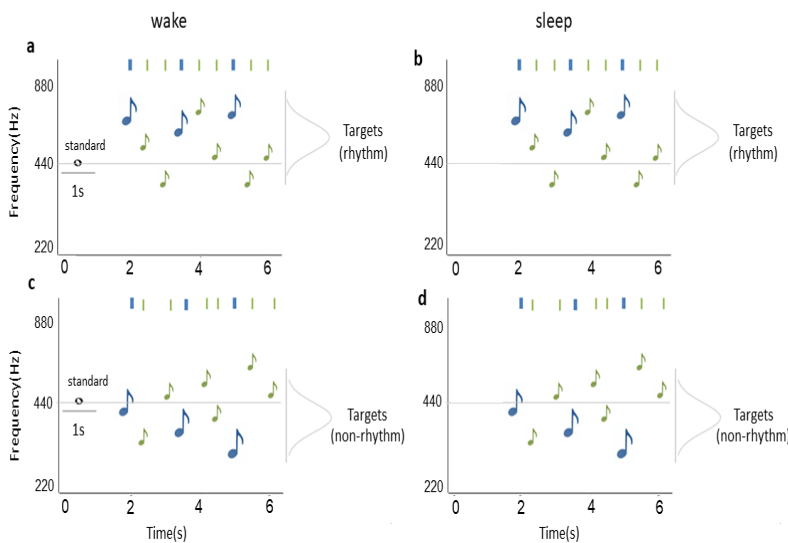


Figure 1. In each trial, subjects should listen to 9 consecutive tones in different amplitude and frequencies, which were also temporally organized either in a periodic (a, b) or an aperiodic manner (c, d). Then they should judge the difference between the frequency of standard tone and the average frequency of the 9 consecutive tones (a, c). While in sleep condition, subjects just passively listened to the stimulus tones (b, d).

RESULTS

During wakefulness (N=16), amplitude information showed a positive modulation on the neural response for each tone, whereas beat information exerted a negative influence with a latency of around 100 to 300ms. The results are well consistent with our previous MEG results (Wang et al., *in prep*). Interestingly, during sleep status (N=17), we observed similar dissociated modulation by amplitude and beat information, but with increased latency.

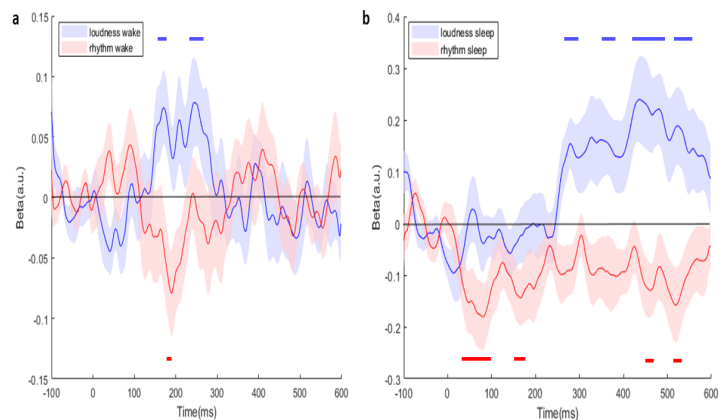


Figure 2. Modulation of loudness and rhythm to the waking (a) and sleeping (b) brain. Loudness showed a positive modulation yet beat information exerted a negative modulation in the two conditions. Red and blue bars mean $p<0.05$ (one sample t-test).

Conclusions

Taken together, our results demonstrate that the brain automatically extracts beat information from auditory inputs to predict the incoming sounds, manifested as the down-modulation effect, consistent with predictive coding theory. Most importantly, the rhythm-based prediction effect also occurs during NREM sleep status. This might constitute a protective mechanism from possible danger during sleep, a status that lacks typical top-down modulations.

References:

- [1] Morillon, B., Schroeder, C. E., & Wyart, V. (2014). Motor contributions to the temporal precision of auditory attention. *Nature Communications* 5.
- [2] Morillon, B., & Baillet, S. (2017). Motor origin of temporal predictions in auditory attention. *Proc Natl Acad Sci U S A*, 114(42), E8913.

Dynamic functional maps capture new features of information integration and consciousness during sleep

EPFL



UNIVERSITÉ
DE GENÈVE

Anjali Tarun^{1,2} [anjali.tarun@epfl.ch], Danyal Wainstein³, Virginie Sterpenich², Lampros Perogamvros², Nikolai Axmacher³, Sophie Schwartz², Dimitri Van De Ville^{1,2}

1 Institute of Bioengineering and Center for Neuroprosthetics, EPFL

2 Faculty of Medicine, University of Geneva

3 Institute of Cognitive Neuroscience, Faculty of Psychology, Ruhr-Universität Bochum

Code Available online!

<https://c4science.ch/source/iCAPs/>

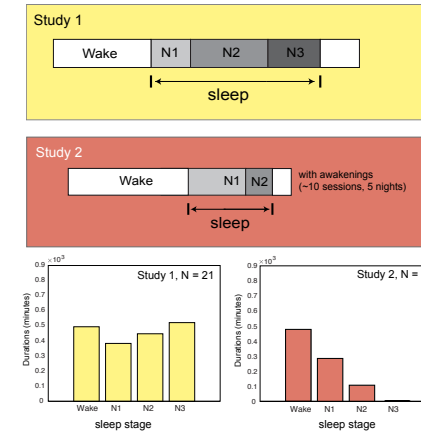
Motivation and Methods

- The brain is continuously active in different mental states (i.e., rest, coma, sleep).
- Resting-state networks are overlapping in space and time and persist at varying durations in different NREM sleep stages.

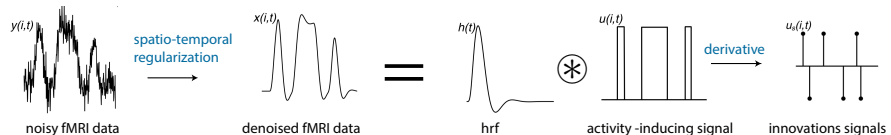
How do these networks interact across vigilance states?

?

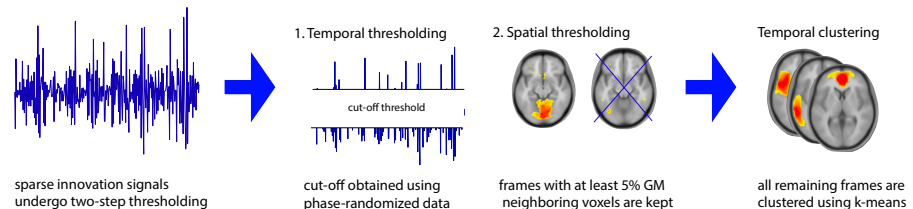
Simultaneous EEG-fMRI Experiments



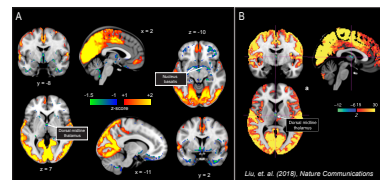
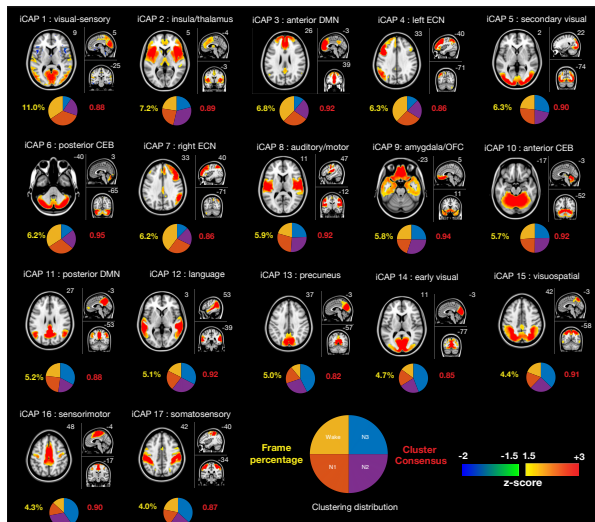
A Total Activation (TA) applied to fMRI data



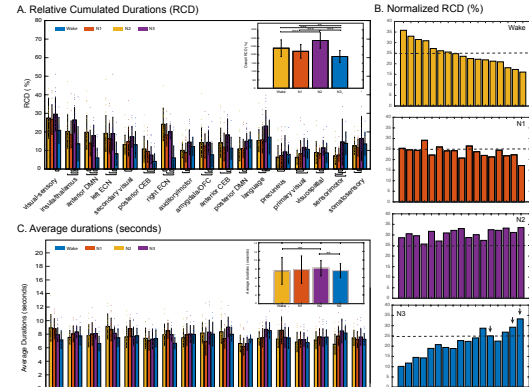
B innovation-driven co-activation patterns (iCAPs) extracted from innovation signals



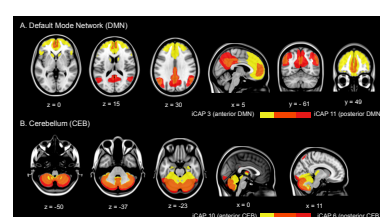
Results



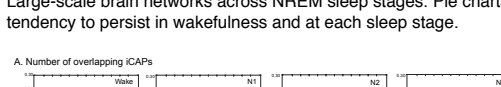
Visual-sensory areas simultaneously activate with negative subcortical regions that are associated with arousal (e.g., basal forebrain).



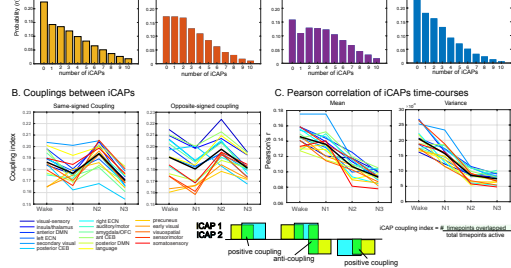
We identified which networks persist at each sleep stage. Networks generally occur the most in N2 and the least in N3. They display continuous bouts of activity for about 5 to 10 seconds.



Cerebellum and default mode networks dissociate into posterior and anterior parts.



Functional connectivity breaks down with increase sleep depth, but networks are surprisingly more coupled in N2 sleep.



Major Findings

- New networks that support the physiological organization of sleep and arousal are captured
- Cerebellum dissociates into posterior and anterior regions, and posterior cerebellum predominates in wake compared to N3
- Contrarily to previously observed strong functional dissociations that accompany the increasing sleep depth, a surge of network activity and cross-network interactions are observed during NREM 2, followed by an abrupt loss of communication in NREM 3
- New features of information integration of consciousness during sleep are captured, and results provide concrete evidence for the presence of unstable yet distributed global synchronization in NREM stage 2

→ Ah, Details are missing :C

- Karahanoglu, F.I. et.al. (2013), 'Total activation: fMRI deconvolution through spatio-temporal regularization', *Neuroimage*, vol 73, pp 121–134
- Karahanoglu, F.I. et.al. (2015), 'Transient brain activity disentangles fMRI resting-state dynamics in terms of spatially and temporally overlapping networks', *Nature Communications*, vol 6, 7751
- D. M. Zöller, et.al. (2018), 'Robust recovery of temporal overlap between network activity using transient-informed spatio-temporal regression,' *IEEE Transactions on Medical Imaging*.
- Bolton, T. A. W., et.al. (2018). Interactions Between Large-Scale Functional Brain Networks are Captured by Sparse Coupled HMMs, *vol 37* (1), 230–240.

A Novel Template-based ICA Approach Reveals Psilocybin-Induced Changes in Thalamic Connectivity

Andrew Gaddis^{a,b,c}, Mary Beth Nebel^{a,d}, Amanda Mejia^e, Stewart Mostofsky^{a,b,d}, Roland Griffiths^{b,c}, Frederick Barrett^{b,c}

^aCenter for Neurodevelopmental and Imaging Research, Kennedy Krieger Institute, Baltimore, MD, USA;

^bJohns Hopkins University School of Medicine, Department of Psychiatry and Behavioral Sciences, Baltimore, MD, USA;

^cCenter for Psychedelic and Consciousness Research, Johns Hopkins University, Baltimore, MD;

^dJohns Hopkins University School of Medicine, Department of Neurology, Baltimore, MD, USA

^eDepartment of Statistics, Indiana University, Bloomington, IN;



Introduction

- The consciousness-altering effects of psychedelic substances such as psilocybin may be due, in part, to changes in thalamocortical connectivity, altering integration of "bottom-up" sensory and "top-down" higher-level cortical processes.
- Most fMRI studies of the acute effects of psychedelics treat the thalamus as one homogenous region, although the thalamus is known to consist of several functionally distinct subnuclei.
- We employ a **novel hierarchical "template" Independent Component Analysis (ICA)** model of resting-state fMRI (rsfMRI) to reliably estimate functional subdivisions of the thalamus at the subject level by leveraging empirical population priors.
- We propose that **intrathalamic functional divisions are distinct, are typically stable/preserved, and may be altered during acute exposure to psilocybin.**

Methods

Template generation (n=20):

- Template ICA assumes that for a predetermined number of regions or ICs, the population mean and variance ("template") are known (diagram 1, below)
- We estimate this template from participants representative of the population of interest.
- 20 volunteers completed a 7-min rsfMRI scan (13M/7F, mean age = 24, SD = 13.4) during screening (at "Baseline-1")
- Spatially constrained group ICA was applied to cleaned, normalized, and smoothed (6-mm FWHM) rsfMRI to generate group-level ICs representing thalamic functional regions.
- To estimate intrasubject variability, we created pseudo test-retest data by splitting each participant's scan in half and then used the group-level maps and dual regression to estimate thalamic ICs for each participant and pseudo-session.
- Resulting participant and pseudo-session IC estimates were used to compute template maps of the mean and between-subject variance for each thalamic component

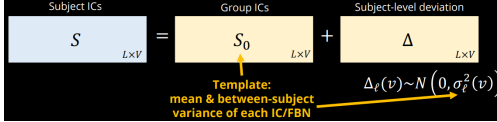


Diagram 1:
Template ICA

Subsequent on-drug and off-drug parcellations (3 total sessions, n=10, diagram 2):

- A subset of the volunteers (n=10) completed three subsequent rsfMRI session (diagram 2):
 - "Baseline-2": Another scan without expectation of drug, several weeks after Baseline-1.
 - 4+ months after Baseline-2: Two, same-day single-blind drug administration conditions:
 - "Placebo"- first session, conducted 110-mins post administration of a placebo capsule
 - "Psilocybin"- second session conducted on the same day as Placebo, but 110-mins post administration of a 10 mg/70 kg oral dose of psilocybin
- Template ICA was applied to each session, utilizing the template maps generated from "Baseline-1" data, resulting in subject-level thalamic parcellations (8 per subject)
- Group-level parcels were created using a two-level winner-take-all approach, with each group-level voxel being assigned to the parcel most common among the subject-level winner-take-all voxel assignments
- Parcel-wise dice coefficients were calculated for subject-level and group-level data

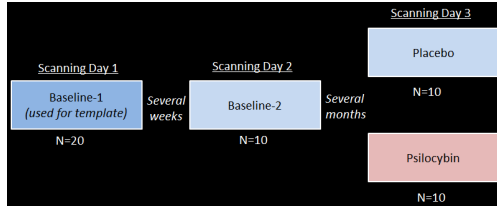


Diagram 2:
Experiment
Design

Thalamic connectivity

- rsfMRI connectivity was computed for each parcel using the CONN toolbox.
- Pearson correlations between each parcel and regions from the probabilistic Harvard-Oxford Atlas were calculated.
- Correlation matrices were transformed using Fisher's r-to-z transformation and were corrected for multiple comparisons using a cluster-level threshold of $p < .05$.

Results: Thalamic parcellations, and concordance across session/state

- Eight thalamic parcels (P1-P8) were estimated for each session (figures 1 and 2).
- Similarity between corresponding group-level parcels was high** (table 1-mean-.67, min-.46).
- Group-level parcels from the psilocybin session were less similar ($p = 0.02$) to baseline than parcels from the placebo session (table 1).
- Participant-level parcels from the psilocybin session were less similar to baseline than parcels from placebo for 3 of the 8 parcels (P3- $p=.033$, P5- $p=.045$, P6- $p=.001$, table 2).
- One parcel (P6) showed particularly reduced congruence ($p = .004$, corrected) when comparing the off-drug state vs acute psilocybin exposure (table 2)**

Baseline 1 vs Placebo								Baseline 2 vs Psilocybin							
P1	P2	P3	P4	P5	P6	P7	P8	P1	P2	P3	P4	P5	P6	P7	P8
0.68387	0.043551	0.033264	0.086176	0.08577	0.017429	0.004619	0.005208	0.669883	0.073248	0.057248	0.031662	0.042735	0.071754	0.019896	0.005102
0.31737	0.611	0.053215	0.054455	0.14561	0.061364	0.020381	0.007453	0.30874	0.60248	0.669793	0.06	0.12598	0.063492	0.023529	0.00984
0.206316	0.023988	0.67158	0.058319	0.018904	0.015905	0.017621	0.01748	0.034384	0.546654	0.044543	0.033457	0.026365	0.004008	0.030303	
0.101082	0.075988	0.073801	0.54911	0.059233	0.073077	0.04048	0.031461	0.021505	0.1321	0.10413	0.45009	0.068053	0.08046	0.032653	0.012425
0.071571	0.10633	0.086053	0.14438	0.059041	0.021742	0.051118	0.024263	0.075397	0.11449	0.028888	0.11189	0.51437	0.058104	0.07717	0.041026
0.17204	0.085106	0.04717	0.059041	0.058392	0.068033	0.021591	0.024159	0.07152	0.058372	0.021012	0.056515	0.042308	0.082102	0.026578	0.74733
0.004435	0.03794	0.064309	0.030303	0.070336	0.02	0.7564	0.053333	0.00885	0.031209	0.056515	0.042308	0.032086	0.028881	0.011494	0.052533
0.009926	0.008696	0.009592	0.041667	0.014493	0.032023	0.73987	0.014851	0.046205	0.033287	0.071307	0.014025	0.050847	0.032086	0.028881	0.011494

Table 1: Dice coefficients comparing the group-level winner-take-all parcels generated from each session. Darker green indicates greater congruence between corresponding parcels.

Parcel Number:	1	2	3	4	5	6	7	8
Mean, Dice Coefficients, OFF/OFF (Baseline-2 vs Placebo)	0.37	0.568	0.503	0.46	0.434	0.564	0.641	0.522
Mean, Dice Coefficients, OFF/ON (Baseline-2 vs Psilocybin)	0.339	0.529	0.452	0.441	0.397	0.501	0.612	0.503
P-values, Dice Coefficients, OFF/OFF vs OFF/ON	0.18	0.164	0.033	0.516	0.045	0.001	0.208	0.197
Adjusted P-values after correction for multiple comparisons	1.440	1.316	0.266	4.127	0.357	0.004	1.667	1.576

Table 2: Mean and p-values (both corrected and uncorrected) for dice coefficients generated from subject-level parcelwise comparisons between sessions

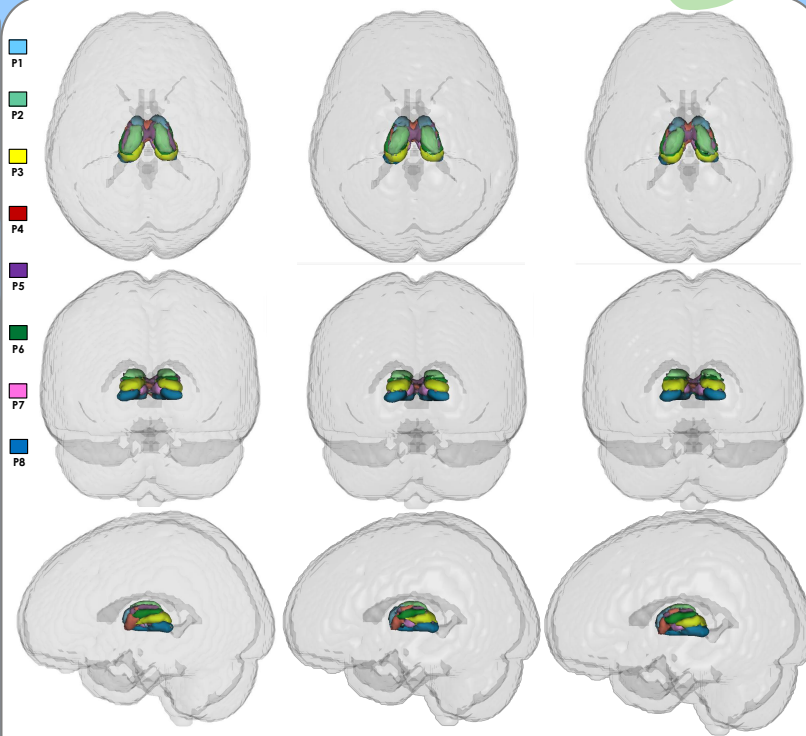


Figure 1: Group-level parcels (n=8) from baseline-1 (left), baseline-2 (middle), placebo (right). P1-cyan, P2-lime green, P3-yellow, P4-red, P5-purple, P6-forest green, P7-pink, P8-navy blue

Results: Thalamic connectivity

Baseline (Baseline-1) thalamic connectivity (table 3, left):

- Most parcels showed highly significant interconnectivity
- Each parcel demonstrates a unique pattern of positive extrathalamic connectivity, and most fall into one of two groups, based on their primary connection to the basal ganglia (BG):
 - Group 1 (P2,P3,P5)** shows primary connectivity with the caudate ($p < .001, .028, <.001$)
 - Group 2 (P6,P7,P8)** shows primary with the pallidum ($p = .01, .02, .001$)
 - Among this group, **P6 is unique in that its primary connectivity is with the Posterior Cingulate (PC) ($p < .001$), the only parcel with primary connectivity outside of the BG.**
- Each parcel also showed diffuse patterns of negative connectivity (not pictured)

Subsequent on-drug and off-drug connectivity for parcel P6 (table 3, right):

- Based on Baseline-1 data above, we selected P6 and its positively connected regions
 - These a priori ROIs included: P1-8, PC, L Pallidum
- There was no statistically significant difference in connectivity between the off-drug states (baseline-2>placebo).**
- There were significant differences in P6 connectivity for psilocybin>placebo, with the pallidum-connected parcels (group 2) showing reduced interparcel connectivity ($p = .0044, .006, .012$), and the pallidum showing reduced connectivity with P8 ($p = 0.045$, table 3, right).**

Baseline-1 (n=20)								Psilocybin>Placebo (n=10)							
Parcel 1	Parcel 2	Parcel 3	Parcel 4	Parcel 5	Parcel 6	Parcel 7	Parcel 8	Parcels 1-6	Parcel 6	Parcel 7	Parcel 8	(Group 2)			
Intrathalamic Connectivity															
Parcel 1		11.19	6.63	4.38	9.24	4.45	2.92								
Parcel 2	11.19		7.17		12.52	8.45	5.9	4.84							
Parcel 3	6.63	7.17		5.14	11.67	12.63	7.15	9.76							
Parcel 4	4.38		5.14		8.37	6.22	13.08	10.08							
Parcel 5	9.24	12.52	11.67	8.37		14.17	10.49	10.4							
Parcel 6	4.45	8.45	12.63	6.22	14.17		10.78	12.21				-3.27	-4.62		
Parcel 7	2.92	5.9	7.15	13.08	10.49	10.78		15.22				-3.27	-4.63		
Parcel 8		4.84	9.76	10.08	10.4	12.21	15.22					-4.62	-4.63		
Extrathalamic Connectivity															
Basal Ganglia															
Caudate (L)	9.77	5.94	3.39			6.51									
Caudate (R)	8.5	4.62				5.07									
Putamen (L)		3.74				4.79									
Putamen (R)	5.91	3.73				4.35						3.77	3.49		
Pallidum (L)		5.38					3.9	3.52	5.03						
Pallidum (R)									3.1	3.93					
Accumbens (L)	4.29				4.56	2.76									
Accumbens (R)	5.38				4.74										
Limbic System															
Amygdala (L)	2.56														
Amygdala (R)	4.88				3.19										
Hippocampus	2.55														
Posterior Cingulate					3.26		2.96	6.37	3.15						
Paracingulate															
Frontal Lobe															

*** Parcel 1 showed diffuse connectivity across frontal lobe ROIs

Table 3: Significant T-values ($p < .05$) for Baseline (left) and Psilocybin>Placebo (Right). Red indicates greater connectivity, blue indicates reduced connectivity. Bold boxes cited in text.

Conclusions/Summary

- Our template ICA-derived intrathalamic functional parcels/nuclei were preserved/stable across off-drug scanning conditions (which were conducted several months apart).
- Parcels were strongly interconnected but showed distinct patterns of extrathalamic connectivity.
- Exposure to psilocybin was associated with acute alteration in otherwise preserved divisions
- Most affected was a parcel with connectivity to the posterior cingulate and the pallidum
- The pallidum showed reduced thalamic connectivity during acute drug exposure, and parcels with primary connectivity to the pallidum became less interconnected.

Catherine Duclos^{1,2}, Danielle Nadin^{1,3}, Yacine Mahid^{1,3}, Alexander Rokos^{1,3}, Mohamed Badawy^{4,5}, Justin Letourneau^{4,5}, Caroline Arbour^{6,7}, Gilles Plourde^{4,5}, Stefanie Blain-Moraes^{1,3}

1. Montreal General Hospital, McGill University Health Center Research Institute, Montreal, QC, Canada
 2. School of Physical and Occupational Therapy, Faculty of Medicine, McGill University, Montreal, QC, Canada
 3. Integrated Program in Neuroscience, Faculty of Medicine, McGill University, Montreal, QC, Canada
 4. Montreal Neurological Hospital and Institute, McGill University Health Center, Montreal, QC

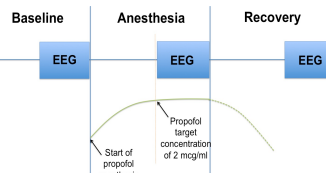
5. Department of Anesthesia, McGill University, Montreal, QC
 6. Centre de recherche, CIUSSS du Nord-de-l'Île-de-Montréal, Montreal, QC
 7. Faculty of Nursing, Université de Montréal, Montreal, QC

INTRODUCTION

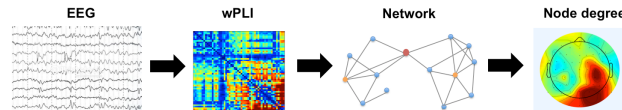
Despite major advances in our understanding of the neural mechanisms of consciousness, clinical assessments still result in the misdiagnosis of disorders of consciousness (DOC) in up to 40% of unresponsive patients. Recent studies have shown that the complexity of cortical response to a direct perturbation of the brain network through transcranial magnetic stimulation provides a reliable index of the brain's capacity for consciousness. Moreover, network neuroscience has shown that a healthy brain adaptively reconfigures its functional network under anesthesia. In healthy individuals, anesthesia induces an anteriorization of alpha network hubs. This study tests the hypothesis that the capacity for this reconfiguration of brain network hubs under anesthesia is indicative of the brain's ability to support consciousness.

METHODS

We applied graph theoretical analysis to high-density electroencephalography (EEG) data recorded in waking, anesthetized, and recovery states in patients with DOC. We recruited 12 DOC patients (42.6 ± 18.0 years old) in the acute (<6 months) or chronic (>6 months) phase following a brain injury. Level of consciousness was assessed behaviorally using the Coma Recovery Scale-Revised within 1h of the EEG recording. We recorded five-minute epochs of 128-channel EEG before, during and after a propofol anesthesia at a target effect site concentration of 2.0 μ g/ml.



Data were bandpass filtered from 0.1 to 50 Hz and re-referenced to an average reference. Non-scalp channels were discarded, and noisy epochs and channels, as well as muscle and non-physiological artifacts, were removed. Alpha (8-14 Hz) networks were constructed using weighted Phase Lag Index (wPLI), and were thresholded using a custom threshold for each participant. The custom threshold was determined by identifying the lowest threshold enabling a minimally-spanning graph during baseline.



The degree of each node in each network was calculated to assess the location of high-degree network hubs. The topographic distribution of hubs was mapped based on the degree of each node within a given network relative to all the other nodes in its network. For all patients, we compared the spatial coherence and topography of alpha network hubs across the three epochs of EEG data.

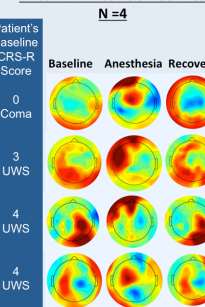
RESULTS

Four patients (1 coma, 3 unresponsive wakefulness syndrome; all acute) had a clear reorganization of alpha network hubs, resembling that of healthy individuals: they showed spatially coherent posterior hubs at baseline, anteriorization of hubs during anesthesia, and a return to spatially coherent posterior hubs after anesthesia.

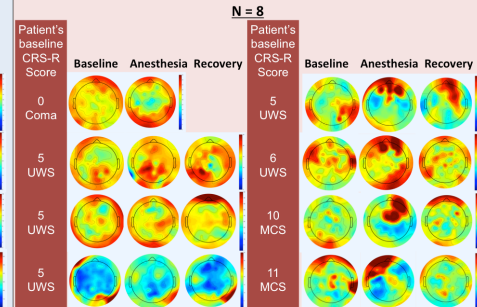
Level of consciousness and phase post-injury

N = 12 PATIENTS	ACUTE	CHRONIC
Coma	2	-
Unresponsive wakefulness syndrome (UWS)	5	3
Minimally Conscious State (MCS)	-	2

RECOVERED CONSCIOUSNESS N = 4



DID NOT RECOVER CONSCIOUSNESS N = 8



Of these four patients, one was presumed to be in locked-in syndrome and irreversibly unconscious, while the other three recovered consciousness in the weeks following the study. Of the eight patients who did not show spatially coherent posterior hubs at baseline and an anteriorization of these hubs under anesthesia, none showed an improvement in the level of consciousness (they deceased or remained in a DOC 6 months later).

CONCLUSION

Our results suggest that the presence of coherent posterior alpha network hubs and their anteriorization under anesthesia may predict recovery of consciousness in unresponsive patients. Importantly, our study suggests that the capacity of a brain network to reorganize following a perturbation is indicative of its potential to recover consciousness. We propose that using anesthesia to assess adaptive network reconfiguration may complement clinical measures for the prognostication of DOC patients.